Taylor & Francis
Taylor & Francis Group

Canadian Journal of Remote Sensing
Journal canadien de télédétection

ISSN: 0703-8992 (Print) 1712-7971 (Online) Journal homepage: www.tandfonline.com/journals/ujrs20

Characterizing the Impact of Non-Stand Replacing Disturbances on LiDAR Based Forest Structure Using a Harmonized Landsat-Sentinel-2 Time-Series

Madison S. Brown, Nicholas C. Coops, Christopher Mulverhill & Alexis Achim

To cite this article: Madison S. Brown, Nicholas C. Coops, Christopher Mulverhill & Alexis Achim (2026) Characterizing the Impact of Non-Stand Replacing Disturbances on LiDAR Based Forest Structure Using a Harmonized Landsat-Sentinel-2 Time-Series, Canadian Journal of Remote Sensing, 52:1, 2631482, DOI: 10.1080/07038992.2026.2631482

To link to this article: https://doi.org/10.1080/07038992.2026.2631482

© 2026 The Author(s). Published by Informa UK Limited, trading as Taylor & Francis Group.

Published online: 05 Mar 2026.

Submit your article to this journal

Article views: 83

View related articles

View Crossmark data

Full Terms & Conditions of access and use can be found at
https://www.tandfonline.com/action/journalInformation?journalCode=ujrs20

CANADIAN JOURNAL OF REMOTE SENSING
2026, VOL. 52, NO. 1, 2631482
https://doi.org/10.1080/07038992.2026.2631482

Taylor & Francis
Taylor & Francis Group

OPEN ACCESS Check for updates

Characterizing the Impact of Non-Stand Replacing Disturbances on LiDAR Based Forest Structure Using a Harmonized Landsat-Sentinel-2 Time-Series

Caractérisation de l'impact des perturbations entraînant des modifications partielles de la structure forestière à l'aide d'une série temporelle harmonisée Landsat-Sentinel-2

Madison S. Brown[a], Nicholas C. Coops[a], Christopher Mulverhill[a], and Alexis Achim[b]

[a]Integrated Remote Sensing Studio, Department of Forest Resource Management, University of British Columbia, Vancouver, BC, Canada; [b]Département des sciences du bois et de la forêt, Université Laval, Québec, QC, Canada

ABSTRACT

Non-stand replacing disturbances (NSRs) are events that do not result in complete removal of forest stands (e.g., insect infestation, windthrow). Forest structural change associated with NSRs can impact forest productivity and health, necessitating the need for both detection of NSR's and characterization of their impact. The increased accessibility of frequent-revisit, medium-resolution satellite imagery, has led to an increase in algorithms designed to detect sub-annual change. The Bayesian Estimator of Abrupt change, Seasonal change, and Trend (BEAST) has shown promise in both detecting NSRs on a sub-annual basis and estimating forest structure changes. This study assesses the impact of NSRs on structure across a dry forest in Western Canada with a case study on aspen leafminer (*Phyllocnistis populiella*) and two-year budworm (*Choristoneura biennis*). Three LiDAR derived forest attributes were modeled (i.e., canopy cover, height and height variability) using BEAST derived predictors variables as inputs (R^2 between 0.5–0.7) and then applied across the study area. Results showed changes in structure over the period of continuous NSRs, including an 11% decline in canopy cover. This approach enables the structural change caused by NSRs to be more rapidly identified, providing practitioners with approaches to better identify areas in need of intervention.

RÉSUMÉ

Les perturbations entraînant des modifications partielles (PEMP) de la structure forestière sont des événements qui ne provoquent pas la disparition complète des peuplements forestiers (p. ex., infestation d'insectes, chablis). Les changements structuraux associés aux PEMP peuvent affecter la productivité et la santé des forêts, d'où la nécessité de détecter ces perturbations et de caractériser leurs impacts. L'accessibilité accrue d'images satellitaires à résolution moyenne et à fréquence de revisite élevée a permis le développement d'algorithmes conçus pour détecter les changements infra-annuels. L'estimateur bayésien des changements abrupts, des changements saisonniers et des tendances (BEAST) s'est révélé prometteur pour la détection des PEMP à l'échelle infra-annuelle et l'estimation des changements structuraux forestiers. Cette étude évalue l'impact des PEMP sur la structure d'une forêt de l'Ouest canadien par une étude de cas portant sur la mineuse du peuplier faux-tremble (Phyllocnistis populiella) et la tordeuse bisannuelle de l'épinette (Choristoneura biennis). Trois attributs forestiers dérivés de données LiDAR (le taux de couvert forestier, la hauteur et sa variabilité) ont été modélisés à l'aide de variables prédictives issues du logiciel BEAST (R^2 compris entre 0,5 et 0,7), puis appliqués à l'ensemble de la zone d'étude. Les résultats ont permis d'identifier une réduction continue par des PEMP pour la période de l'étude, notamment une diminution de 11 % du couvert forestier. L'approche à l'aide de séries temporelles harmonisées Landsat-Sentinel-2 permet d'identifier efficacement les modifications structurelles induites par les PEMP, offrant ainsi aux praticiens des outils pour mieux cibler les zones nécessitant une intervention.

ARTICLE HISTORY
Received 13 June 2025
Accepted 7 February 2026

CONTACT Madison S. Brown madisonsophiabrown@gmail.com

© 2026 The Author(s). Published by Informa UK Limited, trading as Taylor & Francis Group.
This is an Open Access article distributed under the terms of the Creative Commons Attribution License (http://creativecommons.org/licenses/by/4.0/), which permits unrestricted use, distribution, and reproduction in any medium, provided the original work is properly cited. The terms on which this article has been published allow the posting of the Accepted Manuscript in a repository by the author(s) or with their consent.

Introduction

Disturbance plays a critical role in shaping forest structure by altering height, cover and variability, which can in turn impact overall forest dynamics such as species composition, nutrient cycling, and productivity (Atkins et al. 2020; Coops et al. 2020; Hart and Veblen 2015; Trotto et al. 2024; Cohen et al. 2016; Maynard et al. 2014). The impact that specific disturbances have on forest structure is heavily dependent on the disturbance agent. Stand replacing disturbances (SRs) result in complete removal of trees and generally lead to more available growing space resulting in more homogenous, even-aged cohorts (Swanson et al. 2011; Bender et al., 1984). Non-stand replacing disturbances (NSRs) do not result in complete removal of trees and generally occur at a lower severity over a longer period of time (e.g., insect infestation, drought) or at spatially variable intensities over a shorter interval (e.g., windthrow, low-moderate severity fire, frost; Oliver & Larsen, 1996; Payette et al. 1990; Bigler et al. 2005; Hermosilla et al. 2016). This spatial and temporal variability in intensities often leads to more heterogenous stand structures which influences the distribution and quantity of forest biomass (Peng et al. 2011). The overall structural change associated with NSRs can greatly impact both timber supply and ecosystem services, suggesting their detection and characterization is critical to inform future forest health and essential to integrate into forest monitoring programs (Morin Bernard et al. 2023; Woods., 2000; Woods and Kern 2022; Coops et al. 2020).

In Canada, forest inventories document the location, extent, condition, composition, and structure of forested ecosystems in addition to playing a key role in the sustainable management of resources (Tompalski et al. 2021; White et al. 2025). Inventories typically involve the acquisition of aerial imagery that is interpreted to generating a polygonal layer of delineated forest stands which is subsequently assigned various forest attributes (i.e., height, age, canopy cover, etc.) through linkages to ground-based measurements (Gillis and Leckie 1996; Thompson et al. 2007). Enhanced Forest Inventories (EFI) are derived by integrating remote sensing data such as Light detection and ranging (LiDAR) with ground sample data to develop predictive models of forest attributes (e.g., aboveground biomass (t/ha), basal area (m^2/ha), canopy cover (% above 2 m), stem density (n/ha), lorey's height (m), quadratic mean diameter (cm), and stem volume (m^3/ha)) which are typically at a finer spatial resolution than conventional polygon based approaches (Coops et al. 2023; White et al. 2013). However, the cost of LiDAR data (i.e., ≈ $300- 500 CAD per km^2) may present a barrier to its re-acquisition for use in inventories, underscoring the challenge in monitoring structural changes from NSRs (Goodbody et al. 2024).

As a result, information on NSRs is acquired as complementary to these inventory programs and provided through annual provincial or national forest health surveys which are typically undertaken from aircraft or helicopters by forest health specialists and sometimes augmented by field plots (Coleman et al. 2018; Westfall et al., 2019). These surveys are generally updated regularly and provide robust information for long-term monitoring but are deficient when it comes to providing precise locations, impacts on forest structure, or observing sub-annual changes which is useful information to have when implementing mitigation tactics during a growing season. Like conventional forest inventories these surveys consist of polygon-based information and are dependent on expert personnel and equipment to map and observe disturbance patterns. Consequently, linking the occurrence of an NSR to changes in forest structure is challenging (Achim et al. 2022; Coops et al. 2020; Culvenor et al. 2014; Giannetti et al. 2021; Hyyppä et al. 2020).

With the availability of dense time-series of medium-resolution optical satellite imagery (i.e., Landsat and Sentinel-2), there are increased opportunities to detect and monitor NSRs at higher spatial and temporal resolutions compared to conventional polygonal surveys. Through utilizing satellite derived spectral indices, changes in forest condition have been assessed and attributed to a range of NSRs (Hansen and Loveland 2012) including mountain pine beetle (MPB; *Dendroctonus ponderosae*), spruce beetle (*Ips typographus*), and spruce budworm (*Choristoneura fumiferana*; Coops et al. 2006; DeRose et al. 2011; Franklin et al. 2008; Goodwin et al. 2010; Hilker et al. 2009; Meddens et al. 2013). However, these studies mostly focused on detection retrospectively (i.e., after the NSR has reached an epidemic level) rather than continuously (i.e., as the NSR progresses). Algorithms allowing for dense time-series of imagery to be processed (i.e., CCDC, S-CCD), advanced this research enabling

continuous detection of NSRs such as the spongy moth (*Lymantria dispar*; Pasquarella et al. 2017; Ye et al. 2021).

Mulverhill et al. (2025) expanded upon this, utilizing the Bayesian Estimator of Abrupt change, Seasonal change, and Trend (BEAST) algorithm, to detect changes in forest stand structure over time from a dense time-series of optical satellite imagery. To do so, BEAST was used to build annual phenological outputs to a 20-year Landsat and Sentinel-2 time series of spectral indices deriving within-year amplitude, slope, and trend over central Ontario, Canada. Using these spectral outputs, a k-Nearest Neighbor (kNN) approach was then used to predict seven common forest structure attributes (i.e., aboveground biomass (t/ha), basal area (m^2/ha), canopy cover (% above 2 m), stem density (n/ha), lorey's height (m), quadratic mean diameter (cm), and stem volume (m^3/ha); Cover and Hart 1967). Nearest neighbor imputation is a demonstrated methodology to relate satellite-based predictors to LiDAR derived forest attributes (Zald et al., 2014; Matasci et al. 2018). A nearest neighbor imputation (e.g., kNN) has the advantage of allowing all structural attributes to be inputted simultaneously to ensure realistic predictions and has been demonstrated across several studies to inform update of forest inventories (Deo et al. 2017; Fekety et al., 2015; Schleich et al., 2025; Hudak et al. 2008). kNN models generated in Mulverhill et al. (2025) were accurate with relative root mean square errors ranging from 11.47% (canopy cover) to 31.82% (stem volume) demonstrating that data from dense time-series of optical satellite imagery can be used to update LiDAR derived forest inventory information. However, this study only observed these methods in boreal forests and primarily focused on their application to growth and SRs, suggesting a need to test methods on other forest types and undertake a more in-depths study for evaluating application to NSRs.

Brown et al. (2025) demonstrated the BEAST algorithm had potential to detect 93.9% of observed NSR types in a dry interior forest study site ranging from moderate to severe disturbance intensities over an 18-year study period. These results are promising in terms of detection but as the impact of an individual NSR on forest structure varies greatly there is still a need for research to predict the structural change related to NSRs. Hence, the aim of this study is to develop a methodology to assess the impact of NSRs on stand structure across a dry interior site in Western North America. Overall, these methods and results will aid in development of more rapid detection and quantification of NSRs subsequently providing forest managers with better insights into spatiotemporal patterns and structural impacts of NSRs (Achim et al. 2022; Coops et al. 2023; Senf et al. 2017; Trumbore et al. 2015; Trotto et al. 2024). This will be addressed in three objectives: (1) apply methods from Brown et al. (2025) using medium resolution optical satellite data to detect the location of NSRs, (2) use spectral attributes derived from optical satellite data to predict changes to LiDAR derived forest structural metrics, and (3) to develop an approach to match commensurate disturbed and undisturbed stands with similar site characteristics with the purpose of assessing changes in forest structure.

Study location and data

Study location

Our focus is a 1.4 million-ha site in the Interior Plateau of British Columbia, Canada, characterized by dry forest (annual precipitation of 500– 800 mm) and rolling topography (500– 1200 m; Ecological Stratification Working Group 1995; Hessburg and Agee 2005). The most common tree species in the area include Douglas-fir (*Pseudotsuga menziesii*), lodgepole pine (*Pinus contorta*), trembling aspen (*Populus tremuloides)* and white spruce (*Picea glauca;* Ecological Stratification Working Group 1995). The study site covers eight main Biogeoclimatic Ecosystem Classification (BEC) zones and 17 unique subzones; however, the majority resides within the Sub-boreal spruce (dry-warm, moist-warm, moist-hot, moist- cool, wet- warm, very wet cool) and Engelmann spruce- subalpine fir (wet- cool, wet-cold) zones which will be the focus of the study and referred to be here SBS and ESSF (Figure 1).

From 2013–2021, the study site experienced ≈ 589,813 ha of moderate, severe, and very severe NSRs (i.e., those impacting more than 10% of the forest stand area as defined by BC aerial overview survey (BC AOS)) many of which were disturbed in more than one year (Westfall et al., 2019). Disturbances were dominated by fire at a range of severities (47.8%, 281,688 ha) but also included

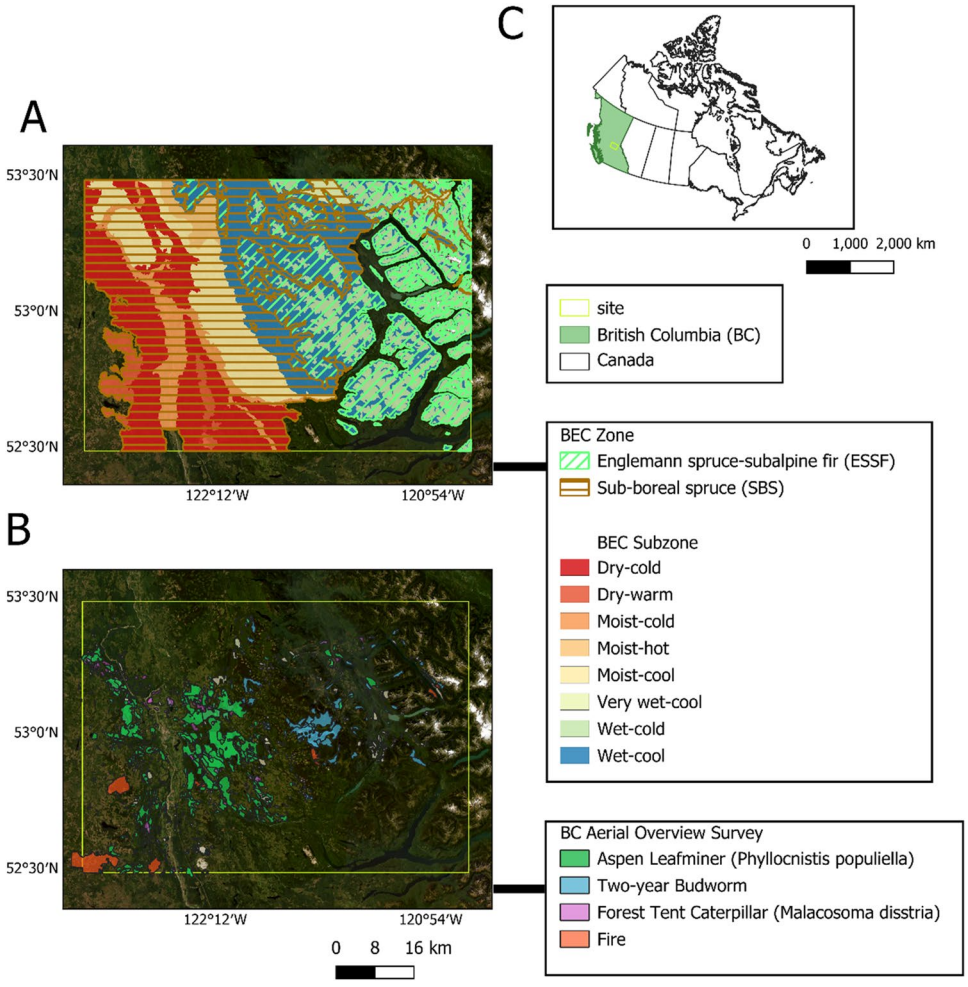

Figure 1. The study area showing (A) Biogeoclimatic Ecosystem Classification (BEC) zones and subzones (Meidinger and Pojar 1991; Pojar et al. 1987), (B) the NSR disturbances as mapped by the BC AOS survey across the study span (2013–2021; Westfall et al, 2019) and (C) the site location within Canada.

aspen leafminer (*Phyllocnistis populiella;* 198,969 ha or 33.7%), two-year budworm (*Choristoneura biennis;* 44,586 ha or ≈ 7.6%), forest tent caterpillar (*Malacosoma disstria*; 44745 ha, 4.6%), and other miscellaneous disturbance agents (37,136 ha, 6.3%) (Figure 1). Aspen leafminer and forest tent caterpillar infestations were highly overlapped in the SBS BEC Zone and were the only non-fire disturbances that reached a severe level. The impact each insect has on forest structure is described in more detail below.

The aspen leafminer is a small moth with a wingspan of about 6 mm. In general, individuals come out of hibernation and reproduce in early spring, concurrent with aspen leaf flushing. After mating, eggs are deposited on new aspen leaves and sheltered by the body of the female moth. Hatching larvae then cut and feed through the leaf, creating serpentine mines (Wagner and Doak 2013). This mining of aspen leaf tissue can cause leaves to turn brown, dry, and eventually drop which reduces the tree's photosynthetic ability, and can potentially reduce canopy cover in leaf-on conditions and reduce growth overall (Furniss and Carolin 1977).

Forest tent caterpillar is a stout-bodied, univoltine moth that impacts deciduous trees. The larvae hatch in the spring as leaves begin to flush and feed for 5–6 weeks before cocooning, with the moths emerging in July (Peters and Despland 2006; Furniss and Carolin 1977). The forest tent caterpillar is one of the most widely distributed and destructive pests throughout North America (Furniss and Carolin 1977). Defoliation during the feeding period can reduce growth, cause top-kill to trees, and in some cases can cause tree mortality (Colasurdo and Despland 2005; Dansereau-Macias et al. 2023).

Data

We utilized four key datasets. The first is a time-series of satellite optical data which was used to detect NSRs. Second, we used a LiDAR dataset to examine the change in forest structure associated with the NSRs and derive topographic variables. Third, we used disturbance polygons acquired from an aerial survey to assess the location, type, and severity of NSRs in the study site. Finally, a set of environmental variables were used to help stratify forest stands in the modeling step. Each of these datasets are explained in detail below.

Medium-resolution optical satellite imagery

Harmonized Landsat Sentinel-2 (HLS) is a virtual satellite constellation which fuses imagery from Landsat 8/9 and Sentinel-2 satellites to produce a spatially and spectrally consistent data product, with a temporal revisit time of 2–3 days, at a 30 m spatial resolution with spectral bands normalized to those of Landsat (Bolton et al. 2018; Claverie et al. 2018; Mulverhill et al. 2025).

HLS v2.0 imagery (L30 and S30) were downloaded for January 1, 2016 - December 31st, 2021 from the NASA Land Processes Distributed Active Archive Center (LP DAAC; NASA 2024). To extend the time-series, all available Landsat 7/8 images from January 1st, 2011 - December 31st, 2015 were downloaded, resampled to the study site, normalized to each other and masked to remove cloud, snow, and water pixels, using the Python package *landsatxplore* (Forget 2023). To balance between reducing temporal noise and interfering with the spectral signature, the masked images were mosaiced into 16-day composites, averaging spectral band values, resulting in a total of 123 images from 2011 to 2021.

LiDAR data

LiDAR data were acquired at a height of 2300 m throughout June- July 2021 using a RIEGL Q1560 sensor (RIEGL 2013). The resulting LiDAR data had a range in point density from 18 to 50 pts/m^2 with an average density of ≈ 25 pts/m^2. Three stand structural metrics were derived from the LiDAR data in addition to site topographic variables: transformed aspect, elevation and slope using the lidR package (Roussel & Auty., 2016; Roussel et al. 2020). 95th percentile of first returns (P95) was included to characterize the impact of NSRs on tree height (Bouvier et al. 2015; Matasci et al. 2018; Nilsson 1996), canopy cover above 2 m (%; Cover > 2 m) was used to capture changes in canopy permeability, and the standard deviation of first returns (SD) was used to describe forest structural complexity, which is useful in describing attributes such as forest health, age, and resilience (Atkins et al. 2020; Lefsky et al. 2005; Matasci et al. 2018; Næsset 2002; Solberg et al. 2006; Vatandaslar et al. 2024)

British Columbia aerial overview survey (BC AOS)

The BC AOS is a provincial landscape-level survey used to detect disturbance events caused by insects, diseases, animals, and abiotic non-anthropogenic factors (Coggins et al. 2008). In its current form, the BC AOS has taken place annually since 1999 (Coggins et al. 2008; Westfall & Ebata, 2019). The survey flight generally occurs between late July to early September, during leaf-on conditions in a fixed wing aircraft. It consists of two experienced observers siting on opposite ends of the plane mapping out visible forest damage, they are later required to combine and agree upon polygon boundaries for there mapped areas to reduce bias. Throughout the survey disturbances are classified by severity, which is defined by percent of the mapped polygon impacted by mortality (Trace: < 1%, Light: 1- 10%, Moderate: 11-29%, Severe: 30-49%, and Very Severe: > 50%). The polygons are also attributed with a disturbance agent which falls into one of five categories: bark beetle, defoliator, abiotic, diseases, or animals. For disturbances that do not cause complete tree mortality such as defoliation or aspen decline, the severity is categorized from light to severe rather than going to very severe and defined by reduction in crown foliage instead of live trees compared to dead trees (Westfall et al, 2019). The BC AOS has limited ground validation protocol and is not generally accurate enough to be directly used for management activities, but rather to be used a guide for regional reporting and finer scale monitoring (Westfall et al., 2019).

Environmental data

Land cover, stand replacing disturbances, and forest age. We utilized data describing land cover, SRs, and forest age from the National Terrestrial Ecosystem Monitoring Systems (NTEMS) which provides national-scale products (Hermosilla et al. 2016; Maltman et al. 2023). In the NTEMS products, stand replacing fire and harvest disturbances were detected using the Normalized Burn Ratio (NBR; Hermosilla et al. 2016; White et al. 2014) derived from Landsat annual best-available-pixel (BAP) composites. The disturbance accuracies ranged from 96.2% for harvesting, to 95.9% for fire and 66.3% for roads (Hermosilla et al. 2016). National land cover was produced using the Virtual Land Cover Engine (VLCE) framework and like disturbances it was derived from Landsat BAP composites, defining numerous cover types in non-vegetated, non-treed, and treed classes (Hermosilla et al. 2018; Hermosilla et al. 2022). The land cover classification layer has an overall accuracy of 77.9% (Hermosilla et al. 2022). Estimated forest age was produced in Maltman et al. (2023) using disturbance events from Hermosilla et al. (2016), the Canadian National Fire database, and Modis Gross Primary Productivity layer. Forest age was calculated for 30 m Landsat pixel in three distinct ways; (1) pixels with direct evidence of stand replacing disturbances (SRs), (2) pixels with evidence of recovery from disturbances, and (3) pixels with no apparent disturbance or recovery where an allometric approach was used to estimate age (Maltman et al. 2023).

Climate. ClimateNA (Version 7.3) was used to generate estimates of climate variables across the study site and to identify disturbed and undisturbed sites with similar conditions. ClimateNA uses a baseline monthly prediction grid for North America, and through a combination of bilinear interpolation and local elevational adjustment, it downscales to match a desired spatial resolution (Wang et al. 2016; Wotherspoon et al. 2024). We used a digital elevation model at a spatial resolution of 30 m as an input to ClimateNA to match the resolution of other data products. Mean Annual Precipitation (MAP), Mean Annual Temperature (MAT), Mean Coldest Month Temperature (MCMT), and Mean Warmest Month Temperature (MWMT) are used in this study.

BEC system. The BEC System is a provincial level classification framework developed to identify and delineate ecologically equivalent regions (MacKenzie and Meidinger 2018). The BEC zones are further divided into subzones based on microclimate, precipitation, and topography (De Cáceres et al. 2015; Meidinger and Pojar 1991). The spatial boundaries of BEC zones and subzones were downloaded to classify similar forest types in the study area (Government of British Columbia, 1991).

Methods

Image processing

Six spectral indices (Normalized Burn Ratio - NBR, Normalized Differential Vegetation Index - NDVI, Tasseled Cap Angle - TCA, Tasseled Cap Wetness - TCW, Tasseled Cap Brightness - TCB, and Tasseled Cap Greeness - TCG) were derived for the 123-image time-series (Table 1). NBR is a normalized ratio between the Near Infrared (NIR) and Shortwave Infrared 2 (SWIR2) and its decline is an indicator of disturbance and/or mortality (Nguyen et al. 2019; Mulverhill et al. 2023). NDVI is representative of vegetation greenness as a function of Red (R) and NIR bands (Morin-Bernard et al. 2023; Pasquarella et al. 2017). The Tasseled Cap Indices (TCA, TCB, TCG, TCW) use a linear transformation between R, Blue (B), Green (G), NIR, Shortwave Infrared 1 (SWIR1), and SWIR2 bands to derive key land surface characteristics (i.e., vegetated area, brightness, vegetation vigor, moisture; Crist and Cicone 1984; Gómez et al. 2011). Subsequently in each image, non-forested pixels, and those pixels having undergone a stand-replacing disturbances (e.g., harvest or severe fire) during the time-series (detected by the annual NTEMS layer) were masked out to ensure only NSRs and undisturbed areas were considered in the study (Figure 2-1).

Spectral variables processing

In order to detect NSRs, the BEAST algorithm was applied to the satellite imagery to generate a smoothed time-series capturing both the seasonality and long-term trend of each non-masked pixel.

Table 1. Spectral indices impacted by NSR used to estimate structural attributes based on HLS data used to derive predictor variables.

Index	Equation	Reference
Normalized Burn Ratio (NBR)	$\frac{NIR-SWIR2}{NIR+SWIR2}$	(Nguyen et al. 2019; Mulverhill et al. 2023)
Normalized Differential Vegetation Index (NDVI)	$\frac{NIR-R}{NIR+R}$	(Morin-Bernard et al. 2023; Pasquarella et al. 2017)
Tasseled Cap Angle (TCA)	$\arctan\left(\frac{TCG}{TCB}\right)$	(Crist and Cicone 1984; Gómez et al. 2011)
Tasseled Cap Brightness (TCB)	$-0.1603B-0.2819G-0.4934R+0.794NIR$ $-0.0002SWIR1-0.1446SWIR2$	(Crist and Cicone 1984; Raab et al. 2019)
Tasseled Cap Greeeness (TCG)	$0.204B+0.4158G+0.5524R+0.5741NIR$ $+0.3124SWIR1+0.2303SWIR2$	(Crist and Cicone 1984; Pasquarella et al., 2021)
Tasseled Cap Wetness (TCW)	$0.0315B+0.2021G+0.3102R+0.1594NIR$ $-0.6806SWIR1-0.6109SWIR2$	(Crist and Cicone 1984; Pasquarella et al. 2017)

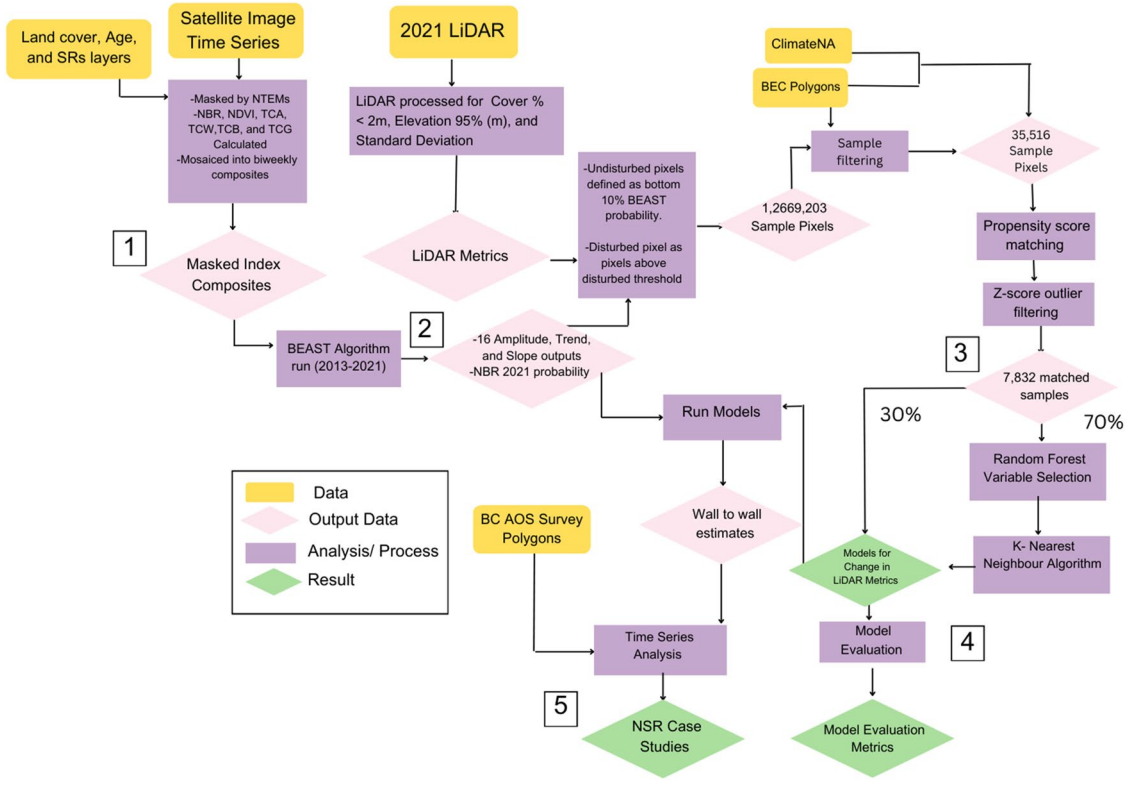

Figure 2. Methods workflow; (1) Model ready imagery, output from *3.1*, (2) Spectral predictor variables, output from *3.2*, (3) Space-for-time matched pixels, output from *3.3*, (4) Generated models, output from *3.4*, and (5) Case studies assessing impact of NSRs, outputs from *3.5*.

In the algorithm, seasonality of each pixel is calculated by using a predicted sinusoidal trend (Mulverhill et al. 2023; Zhao et al. 2019). Two years of data are required to spin up the algorithm hence imagery from 2011 and 2012 was used for this purpose and analysis started from 2013 onwards (Mulverhill et al. 2023; Brown et al. 2025).

From this smoothed time-series, three metrics were calculated to capture phenological variation; the amplitude of sinusoidal curve, the slope of detrended values, and median of detrended values representing overall trend across the epoch (i.e., 365 days). Amplitude provides a baseline for the seasonal conditions of the site, slope captures the more immediate response to disturbances, and trend captures the longer term disturbance trajectory for the season, (Figure 3; Mulverhill et al. 2025). The amplitude, trend, and slope metrics are calculated for epoch prior to the date of interest. For example, the amplitude, slope, and trend on May 31st, 2021 would include all image time-series input from May 31st, 2020 to May 31st, 2021. Amplitude, slope, and trend were calculated for each spectral index, resulting in 18 total metrics.

The probability of disturbance, indicating the degree at which the pixel diverges from the sinusoidal trend in addition to recording the corresponding date of change, was also calculated for each year for NBR (Mulverhill et al. 2023; Zhao et al. 2019). For NSRs in the study site the BEAST probability of disturbance detected ≈ 93.9% of historically mapped NSRs types (Brown et al. 2025). A further threshold ($p = 0.241$) was determined in Brown et al. (2025) allowing for binary classification of the pixels into undisturbed ($p < 0.241$) and disturbed classes ($p > 0.241$; LeDell et al. 2015; Robin et al. 2011; Figure 2-2).

Space-for-time substitution (SFTS)

To quantify the impact of NSRs on the three LiDAR derived metrics of stand structure, we undertook a space-for-time-substitution where disturbed and undisturbed stands in similar environments were compared, on the assumption that *in-situ* site variables (e.g., climate, topography) are determinant in species composition and growth trajectories (Blois et al. 2013; Fukami and Wardle 2005; Likens 1989; Yue et al. 2023). We adapted an approach from Woo et al. (2021) using a distance-weighted propensity score from a series of topographic, and climatic variables. Propensity score $p(X)$ matching (Equation 1) uses a binary logistic function to match treated and untreated units, in this case disturbed and undisturbed pixels, based on defined covariates (β; i.e., topographic, and climatic variables; Austin, 2011; Woo et al. 2021). A binary treatment is used between disturbed pixels and historically undisturbed pixels where $T = 1$ represents the disturbed pixels and $T = 0$ represents the undisturbed pixels. A propensity score is calculated for each pixel and disturbed and undisturbed pixels are matched based on their similarity of propensity scores (Woo et al., 2021). Age using the NTEMs layer was calculated for each of the paired pixels to ensure stands under 10-years were not included (Maltman et al. 2023).

$$p(X) = \Pr(T = 1 \mid X) = E(T \mid X) = \frac{1}{1 + e^{-X\beta}} \qquad \text{(Equation 1)}$$

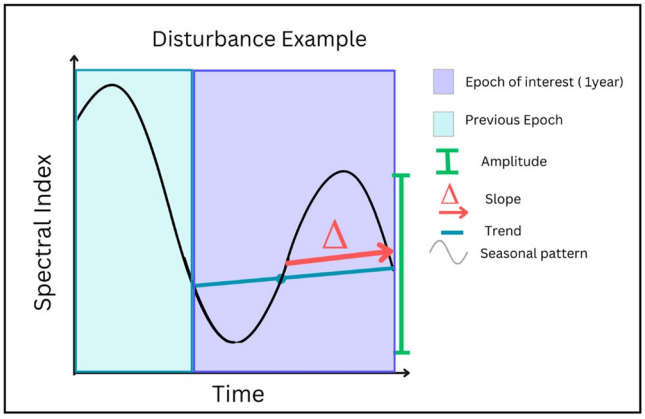

Figure 3. Example of amplitude trend, and slope post disturbance. The amplitude of sinusoidal curve, the slope of detrended values, and median of detrended values representing overall trend across the epoch (365 days).

In order to match pixels, we utilized a suite of matching topographic variables derived from LiDAR and climate variables. We sampled 12,000 disturbed pixels based on the BEAST threshold and matched them to 12,000 undisturbed pixels with similar corresponding environmental conditions (as assessed by the propensity score). We computed Z-scores across these 12,000 samples and removed any pair with a Z- score greater than 2, to ensure highest quality matches, resulting in a total of 7,832 pixels pairs (here after referred to as SFTS pixels). The majority of these pixels had a unique match resulting in a total of 14832 samples (Andrade 2021; Figure 2-3).

Model generation

In order to track changes in the three stand structural metrics over time associated with NSRs our modeling approaches modified from Mulverhill et al. (2025) were as follows. First, the three LiDAR derived structural metrics were directly acquired from the LiDAR point cloud and output as rasters at a 20 m spatial resolution. Then, LiDAR derived structural rasters were resampled (using bilinear interpolation) to match the spatial resolution (30 m) of the BEAST amplitude, slope, and trend for the previous year (June 2020 – May 2021) for all six spectral indices (18 total predictor variables; Hijmans, 2023). Second, in order to account for different forest compositions over the study area, we stratified the SFTS pixels by the two largest BEC zones (ESSF and SBS) and developed individual models for each. For each model 70% of the pixels were randomly assigned and used for model development and the remaining 30% for testing. Third, a Random Forest Regressor model was implemented to select the best spectral variables to be used for each BEC zone model with performance evaluated using k-fold cross validation (Pedregosa et al. 2011). Fourth, the selected variables were imputed into kNN models ($K = 1$) to predict LiDAR structural metrics (Pedregosa et al. 2011; Mulverhill et al. 2025; Berman et al. 2024). Lastly, the models were run on the testing sample for each BEC zone and assessed with standard metrics (coefficient of determination (R^2), root mean square error (RMSE), relative root mean square error (RMSE %), median absolute deviation (MAD), Bias, and Percent Bias (Bias %); Figure 2-4).

The BEAST algorithm was implemented using the *Rbeast* package in R (R Core Team, 2024; Zhao et al. 2019). The Random Forest Regressor and kNN models were implemented using the Python Scikit-learn package (Pedregosa et al., 2011).

Impact of NSR on structure

In order to assess the models' ability to capture landscape-level trends and assess their correspondence to documented NSRs, the models were applied to the entire mosaiced time-series from 2013 to 2021 to provide wall-to-wall predictions. To assess the models' ability to capture landscape level patterns between disturbed and undisturbed areas, SFTS pixels were compared between 2021 LiDAR values and corresponding predicted values. Then matched areas that were flagged as disturbed in a given year were compared annually between 2013 and 2021. Lastly, to assess the models' relationship to documented insect outbreaks, areas impacted consistently by two key NSRs (i.e., aspen leafminer (*Phyllocnistis populiella),* and forest tent caterpillar (*Malacosoma disstria*)), structural values were tracked throughout several growing seasons (Figure 2-5).

Results

Space-for-time substitution (SFTS)

In order to assess the success of the propensity scores to match disturbed and undisturbed pixels we compared the distribution of environmental attribute values, as well as BEAST disturbance probabilities (Figure 4). Propensity scores between the two groups were not significantly different ($p > 0.05$), while BEAST disturbance probability values were statistically significantly different

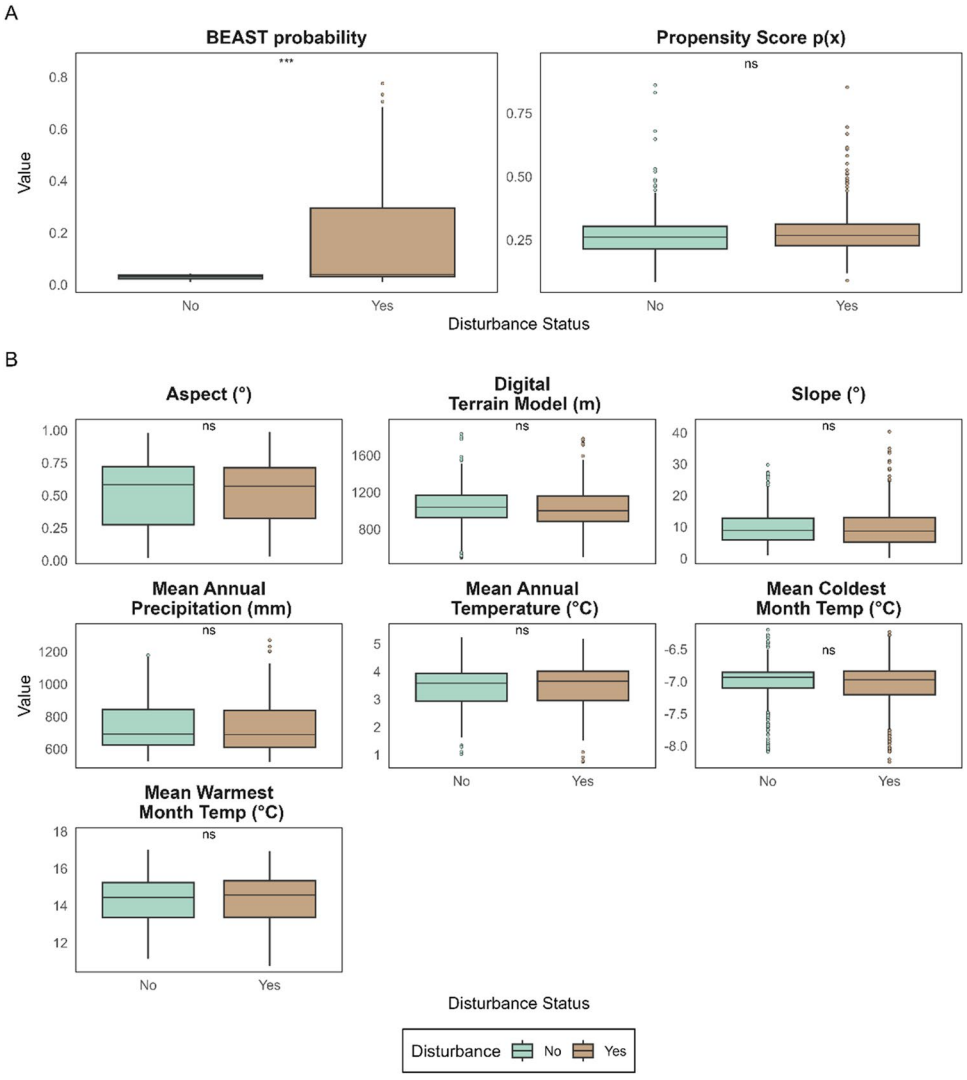

Figure 4. Comparison of disturbed and undisturbed pixel groups of (A) BEAST probability and propensity scores, and (B) Environmental Variables ($p < 0.01$***, $p < 0.05$**, $p < 0.1$*, $p > 0.1$ ns).

($p < 0.05$). Comparisons between environmental attributes also showed no significant differences ($p > 0.05$) between disturbed and undisturbed classes. The mean age of the undisturbed pixels as defined by NTEMS was 55 and 67 for the disturbed pixels with standard deviation of 28 and 38 respectively.

Model evaluation

Models for each BEC zone were developed for the three LiDAR metrics using the attributes derived from the six spectral indices. The Random Forest regressorselected 13 predictor variables for the SBS and 3 for the ESSF (Figure 5). All predictor variables used in the ESSF model Trend-NBR, Trend-TCB, and Amplitude-TCW were used in the SBS model. In both models, the most commonly used indices were NBR, TCB, and TCW. The most common variable type across all spectral indices was the trend variable type. Across both BEC zones, models for Cover > 2 m had the highest R^2 values and lowest RMSE %, followed by SD, and P95 (Figure 6). Models for BEC zone ESSF had a higher average R^2 of ≈ 0.62 compared with SBS of ≈ 0.55 and a lower RMSE % average of ≈ 17.9% ESSF and ≈ 19.62% for SBS. Additionally, MAE, MSE, and RMSE all were all lower in the ESSF BEC zone than in the SBS BEC Zone. Bias % across all models was relatively low, ranging from −0.62– 1.38% (Table 2).

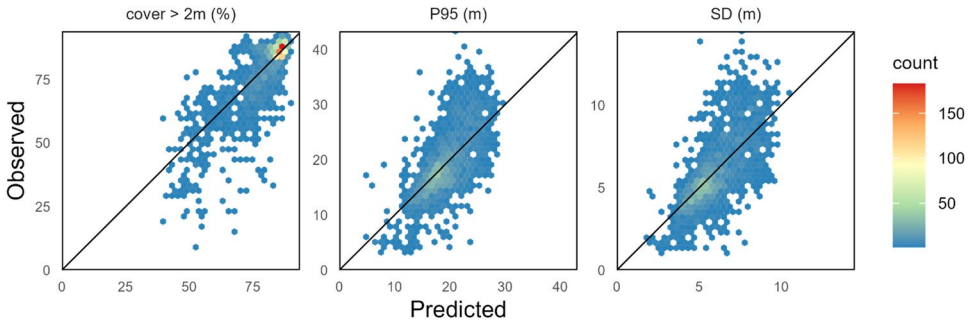

Figure 5. Predicted versus observed structural LiDAR attributes with counts represented in hexagon bins. All BEC zones models have been combined for visualization.

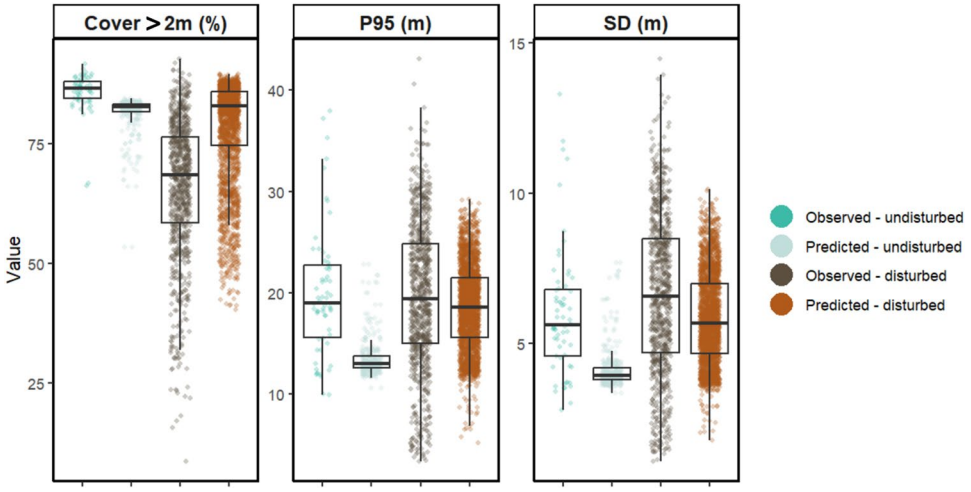

Figure 6. Predicted and observed structural LiDAR attributes for matched disturbed and undisturbed pixel.

Table 2. Model performance by BEC Zone.

Metric	BEC Zone	R^2	MAE	MSE	RMSE	RMSE%	Bias	Bias %
Cover % > 2 m (%)	SBS	0.68	4.79	61.81	7.86	10.01	1.08	1.38
P95 (m)	SBS	0.47	3.30	19.95	4.47	23.18	0.06	−0.62
SD (m)	SBS	0.51	1.11	2.38	1.54	25.63	−0.00	−0.00
Cover > 2 m (%)	ESSF	0.73	3.87	37.79	6.15	8.26	−0.34	−0.46
P95 (m)	ESSF	0.53	2.65	12.53	3.54	21.95	−0.02	−0.15
SD (m)	ESSF	0.60	0.90	1.51	1.23	23.64	0.03	0.59

Application testing

Landscape level pattern

To assess the models' ability to capture landscape level patterns between disturbed and undisturbed areas, SFTS matched pixels were compared between 2021 LiDAR values and corresponding predicted values. Cover > 2 m was higher among the undisturbed category with an average of 86% and 81% for observed and predicted, respectively, compared with an average of 66% and 78% for observed and predicted in the disturbed category, respectively (Figure 6). The pattern in P95 and SD between disturbed and undisturbed categories was also similar between the observed and predicted values. Disturbed pixels had a mean value of 19.61 and 18.58 m for P95 and for SD 6.60 and 5.84 m for observed and predicted samples respectively. Undisturbed pixels had a mean of 17.20 and 13.47 m for P95 and for SD 5.07 and 4.14 m for observed and predicted samples respectively. Both observed and predicted groups showed greater variance and range across all LiDAR metrics for disturbed pixels when compared with undisturbed pixels.

Temporal pattern

Using the BEAST threshold for detection of NSRs cumulatively throughout the study period, 5,338 and 5,448 km^2 (≈ 38% and ≈ 39% of the study site) of disturbed area was detected in the ESSF and SBS BEC zones, respectively. Both BEC zones followed similar patterns in area disturbed, with 2018 being the year with the largest area disturbed (approximately 1,640 and 1,814 km^2 disturbed in ESSF and SBS, respectively). In the SBS, the least amount of NSRs occurred in 2014 (182 km^2), while 2020 had the least amount of disturbance in ESSF (331 km^2; Figure 7). The probability of disturbances did not necessarily track with total disturbed area. For instance, in ESSF from 2013–2017, the median probability increased from ≈0.4 to ≈0.5 and subsequently leveled off for 2018–2020. In SBS, the probability decreased from 2013–2016 from a median value of ≈0.6 to ≈0.4, increased again in 2017 to ≈0.7, then slightly declined in 2018 and 2019, with an increase to ≈0.8 in 2020 (Figure 7).

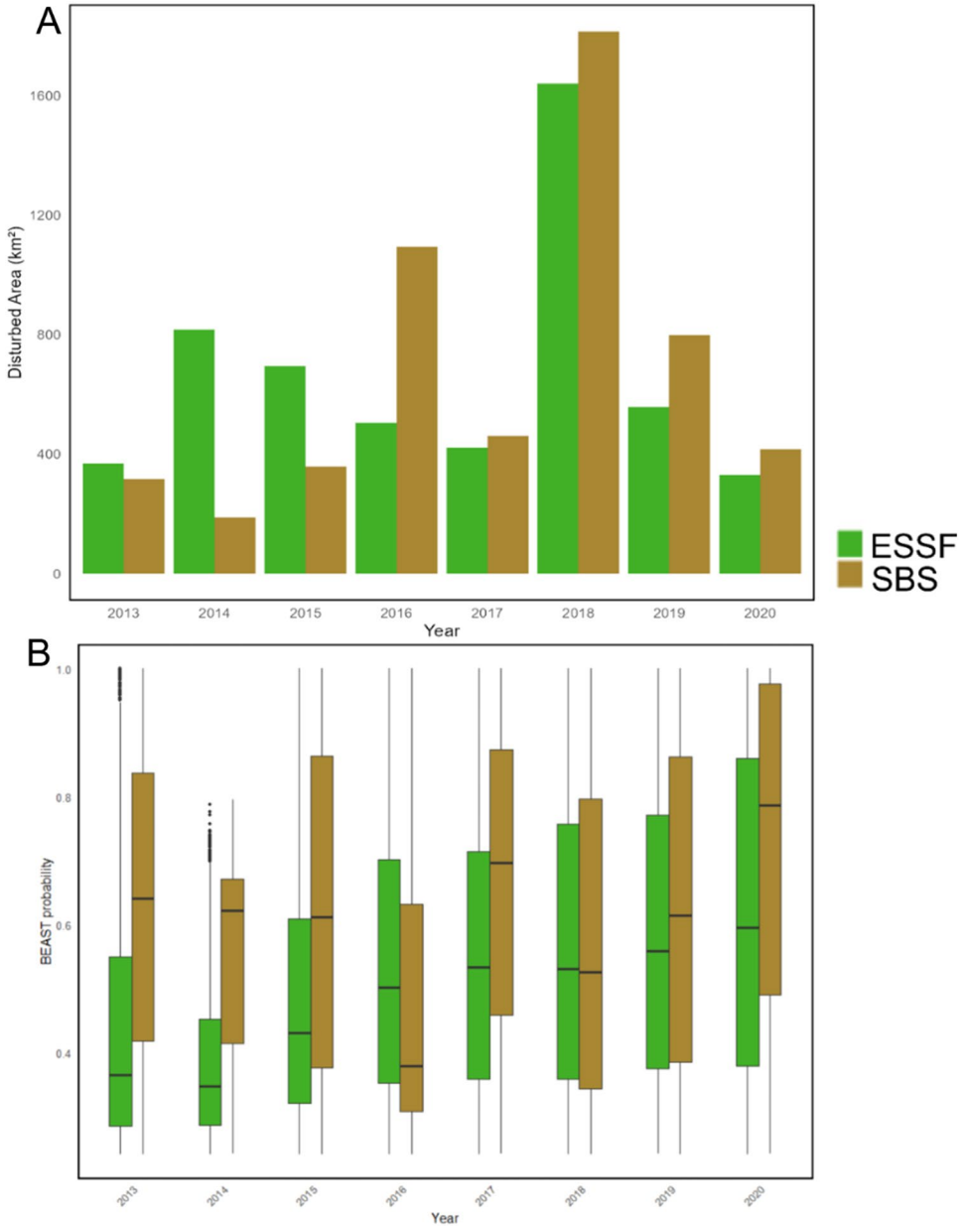

Figure 7. Landscape-level detection of NSR with BEC zone. (A) shows the area detected as disturbed, and (B) shows the distributions of BEAST probability within detected disturbed area.

Trends between predicted structural metrics in SFTS flagged disturbed and undisturbed pixels corresponded to the probability of disturbance particularly for Cover > 2 m. Cover > 2 m for ESSF remained higher for undisturbed areas until probability of disturbance reached its peak median value in 2016 and the Cover > 2 m mean between disturbed and undisturbed pixels converged, and in all years disturbed pixels had a higher P95 and SD (Figures 7 and 8). For SBS, Cover > 2 m remained consistently higher for undisturbed pixels until 2016 when the Cover > 2 m differences became less distinct between the two groups. Conversely, the P95 and SD metrics were not markedly different from each other when comparing the disturbed and undisturbed pixels (Figures 7 and 8). Across the landscape NSRs contributed on average a 0.35% reduction in Cover > 2 m.

Impact of insect damage

In the study area, infestation by aspen leafminer and forest tent caterpillar intensified between July 2016 and 2019. The Cover > 2 m predictions showed high correspondence with this pattern of disturbance (Figure 9). In the area, the mean value of cover > 2 m declined by 11% between 2014 and 2019 with the majority of the decline occurring between 2016 and 2017 as the disturbance intensified. The height-based LiDAR metrics, P95 and SD, showed small declines of an average of 2.1 m and 0.6 m, respectively (Figure 9).

Discussion

Space-for-time substitution (SFTS)

Overall, the SFTS performed well at pairing disturbed and undisturbed pixels with similar site environmental characteristics. There was no statistical difference between the undisturbed and disturbed pixels for any of the environmental variables ($p > 0.05$; Figure 4), and the ecology of paired pixels was similar due to the stratification by BEC zones. However, mean age was younger for undisturbed stands compared to the disturbed stands (i.e., 55 versus 67 years) with a standard deviation of 28 and 38 respectively, suggesting the undisturbed stands represent more even age regrowth, which is shorter and more uniform than the disturbed counterparts. Thus, variables used to match sites were not age sensitive, which could cause challenges in differentiating height-based metrics between disturbed and undisturbed sites.

There are also other factors such as soil quality, long-term disturbance regimes, and anthropogenic impacts that might influence the quality of propensity score matching that we did not fully account for and could be useful to include (Didion et al. 2009; Nlungu-Kweta et al. 2017; Wallace et al. 2021). Additional, field-based measurements could be included to improve and validate the quality of matched areas.

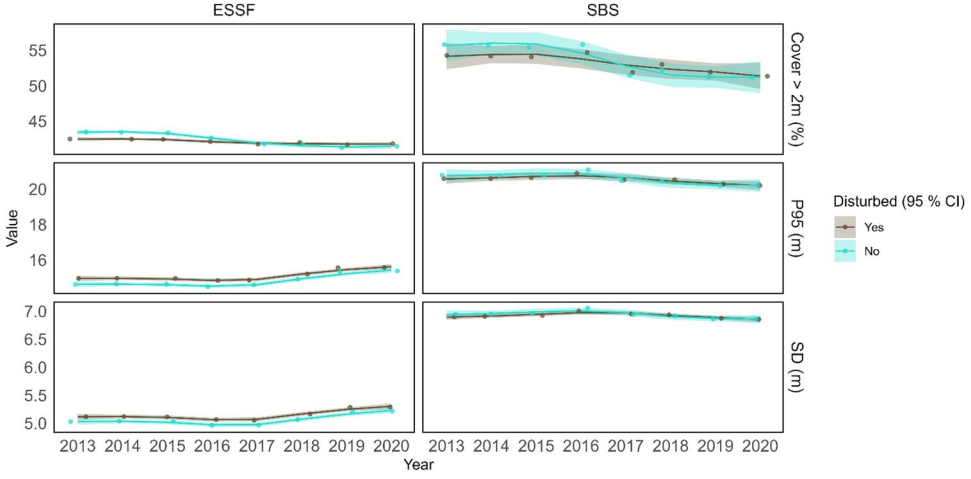

Figure 8. Mean annual estimated forest structural metrics by year (2013–2020) for disturbed and undisturbed matched pixels (smoothed by a Loess regression for visualization purposes with 95% confidence interval (CI)).

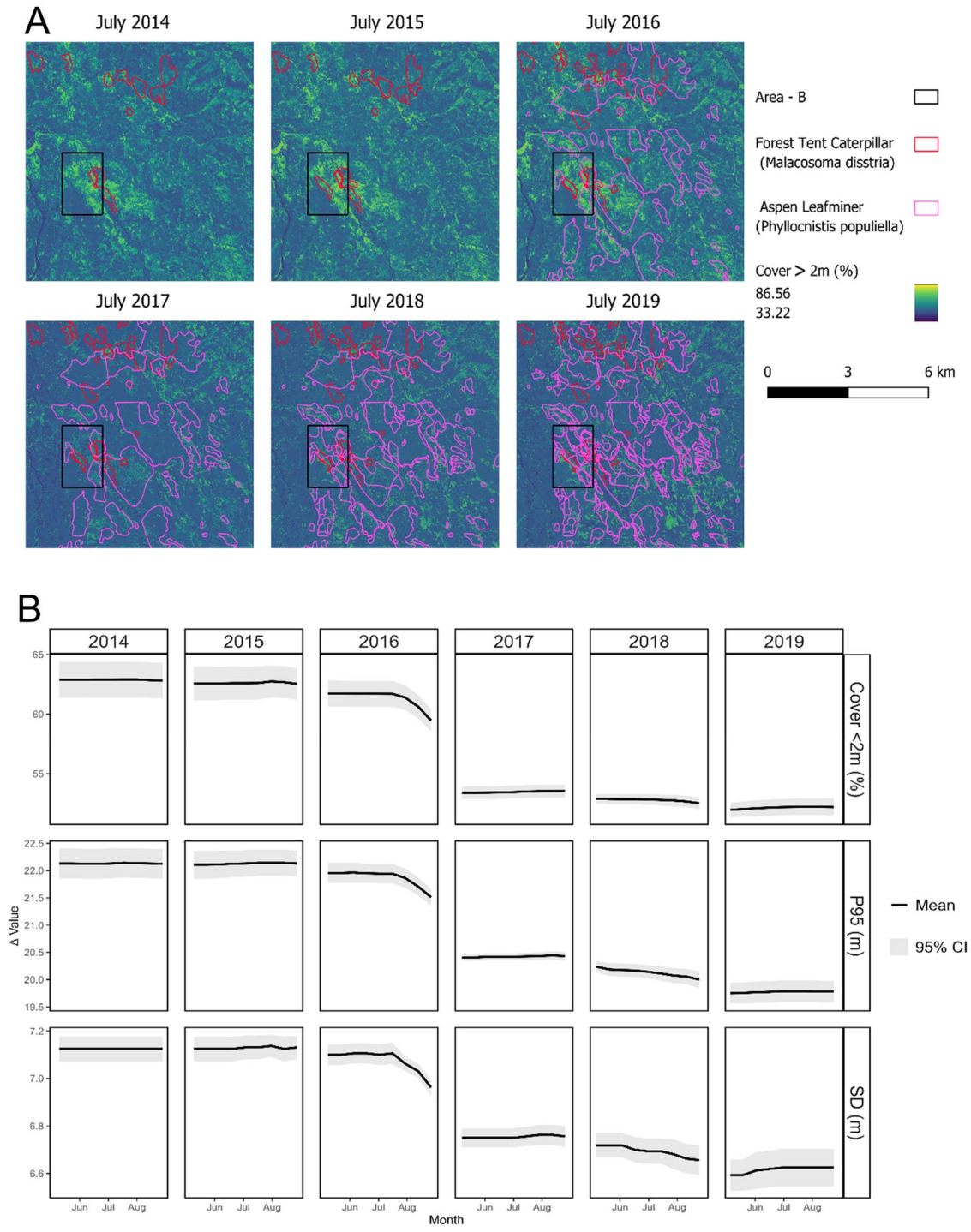

Figure 9. (A) Aspen leafminer *(Phyllocnistis populiella)* and forest tent caterpillar *(Malacosoma disstria)* infestation from July 2014–2019 with model-predicted change in cover > 2 m (%), color scale is representative of cover > 2 m (%) yellow and green areas indicative of lower canopy cover where blue areas representative of higher cover. (B) Mean value of change in LiDAR metrics within AOS case study polygons during growing season with 95% confidence interval (CI).

Model evaluation

The indices utilizing SWIR bands (NBR and TCW) were most commonly selected in both BEC zone models. This is consistent with previous research suggesting SWIR indices were most sensitive to forest structure change, moisture, shadowing, and vegetation density (Jopia et al. 2020; Schroeder et al. 2011) and matched the indices selected in Mulverhill et al. (2025) and Bolton et al. (2020).

The developed models captured the majority of variability with R^2 between 0.47–0.72 and had RMSE % values below 26%. The variability is better captured for Cover > 2 m for both models with R^2 of 0.68 and 0.72 respectively where the height-based metrics ranged from 0.47 –0.60 (Table 2). This is consistent with prior studies showing higher correlation between spectrally-derived predictions for canopy cover metrics compared to height metrics (i.e., height metrics with R^2 between 0.36–0.63 and cover metrics with R^2 between 0.47– 0.77; Matasci et al. 2018; Viana-Soto et al. 2022; Zald et al. 2016).

This better prediction of canopy cover-based metrics compared to height-based metrics is potentially due to oversaturation of the optically derived spectral indices in high canopy cover forests (i.e., once a certain level of point cloud density is reached the indices are no longer sensitive to differences) which is particularly impactful to height metrics causing them consistently to be underpredicted (Bolton et al. 2020; Goetz and Dubayah 2011).

Implications for Forest management and ecology

This research demonstrates the capacity to capture landscape-level trends in NSRs and assess their impact on stand structure over time. From 2013–2020 in disturbed stands, we observed reductions in Cover > 2 m, in stands infested by forest tent caterpillar and aspen leafminer (i.e., an overall 11% decline in 5-years; Figure 9) suggesting the ability of this approach to track the structural change of NSRs in a forest inventory context. This has major forest management implications and provides numerous opportunities to better estimate changes to ecological health and ecosystems services forest provides.

In the context of forest management, identifying NSRs over time and quantifying associated changes in LiDAR-derived forest structure creates new opportunities to target additional monitoring (e.g., manual or finer-scale aerial surveys) in these locations to decrease uncertainty (Coops et al. 2020; White et al. 2025). Additionally, the use of retrospective satellite imagery provides new opportunities for forest management, as users can better interpret the impacts of NSRs on forest structure through time as understanding the historical structural development of an NSR could help guide reactive techniques (e.g., salvage harvesting).

On the ecological front, high-temporal-frequency forest structure estimates can inform decision-making in numerous areas. For instance, caribou habitat is highly sensitive to disturbance, as associated structural changes can increase visibility to predators and reduce food availability (Kerr and Deguise 2004; Maltman et al. 2024). Moreover, forest structure post-disturbance is important in monitoring fire risk and can impact post-fire recovery, as deadfall and other debris can lead to increased fire fuels and alter soil quality (Andersen et al. 2005; Hagmann et al. 2021; Smith-Tripp et al. 2024). There is also evidence that structural factors such as canopy height and canopy cover can affect overall forest resilience to drought, further necessitating the importance of monitoring forest structure (Ma et al. 2023).

Future work

Overall, this study demonstrated the potential for continuous detection and characterization of a variety of NSRs providing a foundation for integrating NSRs into forest inventories throughout Canada. Suggesting there is potential for methods from this work to track historical NSRs (i.e., specifically insect outbreaks) and predicting future likelihood of their occurrence. For example, Srivastava and Carroll (2023) used climate variables and tree species proportions to predict the likelihood of a MPB outbreak using polygonal aerial survey data as validation. Results from this work could be used to supplement aerial survey data providing higher frequency, finer scale NSR locations along with associated structural change which could aid in the development of more precise and higher frequency predictions of future outbreaks.

There is also a demonstrated need for research beyond landscape-level detection and characterization. Updating a forest inventory for the occurrence and estimated structural change of NSRs serves

as the initial tool in implementing better adaptation and mitigation strategies. Once an NSR has been identified and impact on forest structure assessed, further validation, acquisitions of remotely piloted aerial systems, aircraft-based images or LiDAR data can be planned to provide more detailed information on effects of NSRs over time (Coops et al. 2020).

However, with broader applications further optimization of these methods to other forest types and regions is required. First, when developing models for the multiple areas there is a need to consider the impact of spatial autocorrelation, on the model performance and overall results may be poorer than presented here if spatial autocorrelation is present in the datasets. Further, model assessment could include a block-base approach separating the observations into different sets using their coordinates (Roberts et al. 2017), or spatial filtering approach to removing observations for points with a certain distance of each other (Boria et al., 2014).

Second, sub-annual, fine spatial scale validation data such as higher spatial and temporal resolution surveys, field measurements or additional finer-scale data acquisition in focused sites is needed. Finer-scale NSR validation could be used in tandem with a second LiDAR acquisition enabling more NSR specific LiDAR structural metrics to be selected for prediction. Additionally, as this work was conducted on a dry interior area in Western Canada on NSRs that were specific to this region, there is a need to test these methods on different regions and NSR types.

Lastly, the emergence of longer time-series of higher resolution multispectral satellite imagery (e.g., Sentinel-2 with 10 m resolution, starting in late 2015) may also provide better detection and structural characterization of finer-scale NSRs (Kempeneers and Soille 2017).

Conclusion

NSRs act as a key driver in forest structure and composition, shifting attributes such as biomass dynamics and impacting timber supply and ecosystem services (Peng et al. 2011; Woods and Kern 2022). Therefore, to anticipate the future health and condition of forests, it is critical to have a continuously updating inventory framework to quantify the impact of NSRs (Coops et al. 2023). This study demonstrated the ability of a continuous change detection algorithm to be applied to long-term optical satellite observations of a dry interior forest to continuously detect NSRs through time and space, and assessed structural changes. In doing this allowing for the structural changes attributed to a variety of NSRs to be tracked over the landscape at a sub-annual scale increasing the opportunities for early detection, assessment, and mitigation strategies to be implemented.

Acknowledgements

This analysis was conducted on the ancestral and unceded territories of the xʷməθkʷəy̓əm (Musqueam), Dënéndeh and Tŝilhqot'in Nen people. This research was funded by a NSERC Alliance project Silva21 NSERC ALLRP 556265–20, and a Class Grant from the Canadian Space Agency (22IUCLAV14). Grantee Prof. Alexis Achim. We would like to thank Dr. Jeanine Rhemtulla, Elaine Ye, and Florence Leduc for their additional feedback.

References

Achim, A., Moreau, G., Coops, N.C., Axelson, J.N., Barrette, J., B′ Edard, S., Byrne, K.E., *et al.* 2022. "The changing culture of silviculture." *Forestry: An International Journal of Forest Research*, Vol. 95 (No. 2): pp. 143–152. doi:10.1093/forestry/cpab047.

Andersen, H.-E., McGaughey, R.J., and Reutebuch, S.E. 2005. "Estimating forest F fuel parameters using LIDAR data." *Remote Sensing of Environment*, Vol. 94 (No. 4): pp. 441–449. doi:10.1016/j.rse.2004.10.013.

Andrade, C. 2021. "Z Scores, Standard Scores, and Composite Test Scores Explained." *Indian Journal of Psychological Medicine*, Vol. 43 (No. 6): pp. 555–557. doi:10.1177/02537176211046525.

Atkins, J.W., Bond-Lamberty, B., Fahey, R.T., Haber, L.T., Stuart-Haëntjens, E., Hardiman, B.S., LaRue, E., *et al.* 2020. "Application of multidimensional structural characterization to detect and describe moderate forest disturbance." *Ecosphere*, Vol. 11 (No. 6): pp. e03156. doi:10.1002/ecs2.3156.

Berman, E.E., Coops, N.C., Robere-McGugan, G., Sinclair, I., McCartney, G., and Achim, A. 2024. "Updating forest stand inventories: integration of photo-interpreted and airborne laser scanning forest attributes using generic region merging segmentation and kNN imputation." *Canadian Journal of Remote Sensing*, Vol. 50 (No. 1): pp. 2391319. doi:10.1080/07038992.2024.2391319.

Bigler, C., Kulakowski, D., and Veblen, T.T. 2005. "Multiple disturbance interactions and drought influence fire severity in rocky mountain subalpine forests." *Ecology*, Vol. 86 (No. 11): pp. 3018–3029. doi:10.1890/05-0011.

Blois, J.L., Williams, J.W., Fitzpatrick, M.C., Jackson, S.T., and Ferrier, S. 2013. "Space can substitute for time in predicting climate-change effects on biodiversity." *Proceedings of the National Academy of Sciences of the United States of America*, Vol. 110 (No. 23): pp. 9374–9379. doi:10.1073/pnas.1220228110.

Bolton, D.K., Tompalski, P., Coops, N.C., White, J.C., Wulder, M.A., Hermosilla, T., Queinnec, M., *et al.* 2020. "Optimizing Landsat time series length for regional mapping of lidar-derived forest structure." *Remote Sensing of Environment*, Vol. 239: pp. 111645. doi:10.1016/j.rse.2020.111645.

Bolton, D.K., White, J.C., Wulder, M.A., Coops, N.C., Hermosilla, T., and Yuan, X. 2018. "Updating stand-level forest inventories using airborne laser scanning and Landsat time series data." *International Journal of Applied Earth Observation and Geoinformation*, Vol. 66: pp. 174–183. doi:10.1016/j.jag.2017.11.016.

Bouvier, M., Durrieu, S., Fournier, R.A., and Renaud, J.-P. 2015. "Generalizing predictive models of forest inventory attributes using an area-based approach with airborne LiDAR data." *Remote Sensing of Environment*, Vol. 156: pp. 322–334. doi:10.1016/j.rse.2014.10.004.

Brown, M.S., Coops, N.C., Mulverhill, C., and Achim, A. 2025. "Detection of non-stand replacing disturbances (NSR) using Harmonized Landsat-Sentinel-2 time series." *ISPRS Journal of Photogrammetry and Remote Sensing*, Vol. 220: pp. 264–276. doi:10.1016/j.isprsjprs.2024.12.014.

Claverie, M., Ju, J., Masek, J.G., Dungan, J.L., Vermote, E.F., Roger, J.-C., Skakun, S.V., and Justice, C. 2018. "The Harmonized Landsat and Sentinel-2 surface reflectance data set." *Remote Sensing of Environment*, Vol. 219: pp. 145–161. doi:10.1016/j.rse.2018.09.002.

Coggins, S.B., Wulder, M.A., Coops, N.C., and White, J.C. 2008. "Linking survey detection accuracy with ability to mitigate populations of mountain pine beetle." *The Forestry Chronicle*, Vol. 84 (No. 6): pp. 900–909. doi:10.5558/tfc84900-6.

Cohen, W.B., Yang, Z., Stehman, S.V., Schroeder, T.A., Bell, D.M., Masek, J.G., Huang, C., and Meigs, G.W. 2016. "Forest disturbance across the conterminous United States from 1985–2012: The emerging dominance of forest decline." *Forest Ecology and Management*, Vol. 360: pp. 242–252. doi:10.1016/j.foreco.2015.10.042.

Colasurdo, N., and Despland, E. 2005. "Social cues and following behavior in the forest tent caterpillar." *Journal of Insect Behavior*, Vol. 18 (No. 1): pp. 77–87. doi:10.1007/s10905-005-9348-6.

Coleman, T.W., Graves, A.D., Heath, Z., Flowers, R.W., Hanavan, R.P., Cluck, D.R., and Ryerson, D. 2018. "Accuracy of aerial detection surveys for mapping insect and disease disturbances in the United States." *Forest Ecology and Management*, Vol. 430: pp. 321–336. doi:10.1016/j.foreco.2018.08.020.

Coops, N.C., Johnson, M., Wulder, M.A., and White, J.C. 2006. "Assessment of QuickBird high spatial resolution imagery to detect red attack damage due to mountain pine beetle infestation." *Remote Sensing of Environment*, Vol. 103 (No. 1): pp. 67–80. doi:10.1016/j.rse.2006.03.012.

Coops, N.C., Shang, C., Wulder, M.A., White, J.C., and Hermosilla, T. 2020. "Change in forest condition: Characterizing non-stand replacing disturbances using time series satellite imagery." *Forest Ecology and Management*, Vol. 474: pp. 118370. doi:10.1016/j.foreco.2020.118370.

Coops, N.C., Tompalski, P., Goodbody, T.R.H., Achim, A., and Mulverhill, C. 2023. "Framework for near real-time forest inventory using multi source remote sensing data." *Forestry: An International Journal of Forest Research*, Vol. 96 (No. 1): pp. 1–19. doi:10.1093/forestry/cpac015.

Cover, T., and Hart, P. 1967. "Nearest neighbor pattern classification." *IEEE Transactions on Information Theory*, Vol. 13 (No. 1): pp. 21–27. doi:10.1109/TIT.1967.1053964.

Crist, E.P., and Cicone, R.C. 1984. "A physically-based transformation of Thematic Mapper data—the TM Tasseled Cap." *IEEE Transactions on Geoscience and Remote Sensing*, Vol. GE-22 (No. 3): pp. 256–263. doi:10.1109/TGRS.1984.350619.

Culvenor, D., Newnham, G., Mellor, A., Sims, N., and Haywood, A. 2014. "Automated in-situ laser scanner for monitoring forest leaf area index." *Sensors (Basel, Switzerland)*, Vol. 14 (No. 8): pp. 14994–15008. doi:10.3390/s140814994.

Dansereau-Macias, É., Despland, E., and Handa, I.T. 2023. "Decreased soil microbial biomass and changed microbial community composition following a defoliation event by the forest tent caterpillar." *Forests*, Vol. 14 (No. 4): pp. 792. doi:10.3390/f14040792.

De Cáceres, M., Chytrý, M., Agrillo, E., Attorre, F., Botta-Dukát, Z., Capelo, J., Czúcz, B., *et al.* 2015. "A comparative framework for broad-scale plot-based vegetation classification." *Applied Vegetation Science*, Vol. 18 (No. 4): pp. 543–560. doi:10.1111/avsc.12179.

Deo, R.K., Russell, M.B., Domke, G.M., Woodall, C.W., Falkowski, M.J., and Cohen, W.B. 2017. "Using Landsat time-series and LiDAR to inform aboveground forest biomass baselines in Northern Minnesota, USA." *Canadian Journal of Remote Sensing*, Vol. 43 (No. 1): pp. 28–47. doi:10.1080/07038992.2017.1259556.

DeRose, R.J., Long, J.N., and Ramsey, R.D. 2011. "Combining dendrochronological data and the disturbance index to assess Engelmann spruce mortality caused by a spruce beetle outbreak in southern Utah, USA." *Remote Sensing of Environment*, Vol. 115 (No. 9): pp. 2342–2349. doi:10.1016/j.rse.2011.04.034.

Didion, M., Kupferschmid, A.D., and Bugmann, H. 2009. "Long-term effects of ungulate browsing on forest composition and structure." *Forest Ecology and Management*, Vol. 258: pp. S44–S55. doi:10.1016/j.foreco.2009.06.006.

Ecological Stratification Working Group 1995. A National Ecological Framework for Canada Agriculture and Agri-Food Canada and Environment Canada, Research Branch, Centre for Land and Biological Resources Research, and Environment Canada, State of the Environment Directorate, Ecozone Analysis Branch, Ottawa, Ont (Report and national map at 1:7 500 000 scale)

Fekety, P.A., Falkowski, M.J., and Hudak, A.T. 2015. "Temporal transferability of LiDAR-based imputation of forest inventory attributes." *Canadian Journal of Forest Research*, Vol. 45 (No. 4): pp. 422–435. doi:10.1139/cjfr-2014-0405.

Forget, Y. 2023. Landsatxplore (1.0.3) [Software]. PyPI. https://pypi.org/project/landsatxplore/

Franklin, S.E., Fan, H., and Guo, X. 2008. "Relationship between Landsat TM and SPOT vegetation indices and cumulative spruce budworm defoliation." *International Journal of Remote Sensing*, Vol. 29 (No. 4): pp. 1215–1220. doi:10.1080/01431160701730136.

Fukami, T., and Wardle, D.A. 2005. "Long-term ecological dynamics: Reciprocal insights from natural and anthropogenic gradients." *Proceedings of the Royal Society B: Biological Sciences*, Vol. 272 (No. 1577): pp. 2105–2115. doi:10.1098/rspb.2005.3277.

Furniss, R. L., and Carolin, V. M. 1977. "Western Forest Insects" Aspen Bibliography. Paper 4906. https://digitalcommons.usu.edu/aspen_bib/4906

Gillis, M.D., and Leckie, D.G. 1996. "Forest inventory update in Canada." *The Forestry Chronicle*, Vol. 72 (No. 2): pp. 138–156. doi:10.5558/tfc72138-2.

Giannetti, F., Pecchi, M., Travaglini, D., Francini, S., D'Amico, G., Vangi, E., Cocozza, C., and Chirici, G. 2021. "Estimating VAIA windstorm damaged forest area in Italy using time series Sentinel-2 imagery and continuous change detection algorithms." *Forests*, Vol. 12 (No. 6): pp. 680. doi:10.3390/f12060680.

Goetz, S., and Dubayah, R. 2011. "Advances in remote sensing technology and implications for measuring and monitoring forest carbon stocks and change." *Carbon Management*, Vol. 2 (No. 3): pp. 231–244. doi:10.4155/cmt.11.18.

Gómez, C., White, J.C., and Wulder, M.A. July 2011. "Characterizing the state and processes of change in a dynamic forest environment using hierarchical spatio-temporal segmentation." *Remote Sensing of Environment*, Vol. 115 (No. 7): pp. 1665–1679. doi:10.1016/j.rse.2011.02.025.

Goodbody, T.R.H., Coops, N.C., Irwin, L.A.K., Armour, C.C., Saunders, S.C., Dykstra, P., Butson, C., and Perkins, G.C. 2024. "Integration of Airborne Laser Scanning data into forest ecosystem management in Canada: Current status and future directions." *The Forestry Chronicle*, Vol. 100 (No. 2): pp. 238–258. doi:10.5558/tfc2024-014.

Goodwin, N.R., Magnussen, S., Coops, N.C., and Wulder, M.A. 2010. "Curve fitting of time-series Landsat imagery for characterizing a mountain pine beetle infestation." *International Journal of Remote Sensing*, Vol. 31 (No. 12): pp. 3263–3271. doi:10.1080/01431160903186277.

Government of British Columbia n.d. *BEC WEB*. www.for.gov.bc.ca. https://www.for.gov.bc.ca/hre/becweb/resources/maps/

Hagmann, R.K., Hessburg, P.F., Prichard, S.J., Povak, N.A., Brown, P.M., Fulé, P.Z., Keane, R.E., *et al.* 2021. "Evidence for widespread changes in the structure, composition, and fire regimes of western North American forests." *Ecological Applications: a Publication of the Ecological Society of America*, Vol. 31 (No. 8): pp. e02431. doi:10.1002/eap.2431.

Hansen, M.C., and Loveland, T.R. 2012. "A review of large area monitoring of land cover change using Landsat data." *Remote Sensing of Environment*, Vol. 122: pp. 66–74. doi:10.1016/j.rse.2011.08.024.

Hart, S.J., and Veblen, T.T. 2015. "Detection of spruce beetle-induced tree mortality using high- and medium-resolution remotely sensed imagery." *Remote Sensing of Environment*, Vol. 168: pp. 134–145. doi:10.1016/j.rse.2015.06.015.

Hermosilla, T., Bastyr, A., Coops, N.C., White, J.C., and Wulder, M.A. 2022. "Mapping the presence and distribution of tree species in Canada's forested ecosystems." *Remote Sensing of Environment*, Vol. 282: pp. 113276. doi:10.1016/j.rse.2022.113276.

Hermosilla, T., Wulder, M.A., White, J.C., Coops, N.C., and Hobart, G.W. 2018. "Disturbance-informed annual land cover classification maps of Canada's forested ecosystems for a 29-year Landsat time series." *Canadian Journal of Remote Sensing*, Vol. 44 (No. 1): pp. 67–87. doi:10.1080/07038992.2018.1437719.

Hermosilla, T., Wulder, M.A., White, J.C., Coops, N.C., Hobart, G.W., and Campbell, L.B. 2016. "Mass data processing of time series Landsat imagery: Pixels to data products for forest monitoring." *International Journal of Digital Earth*, Vol. 9 (No. 11): pp. 1035–1054. doi:10.1080/17538947.2016.1187673.

Hessburg, P. F., and Agee, J. K. 2005. *Dry forests and wildland fires of the inland Northwest USA: Contrasting the landscape ecology of the pre-settlement and modem eras*.

Hijmans, R. J. 2023. Terra: Spatial Data Analysis (1.7–3). Computer software; https://cran.r-project.org/package=terra.

Hilker, T., Wulder, M.A., Coops, N.C., Linke, J., McDermid, G., Masek, J.G., Gao, F., and White, J.C. 2009. "A new data fusion model for high spatial- and temporal-resolution mapping of forest disturbance based on Landsat and MODIS." *Remote Sensing of Environment*, Vol. 113 (No. 8): pp. 1613–1627. doi:10.1016/j.rse.2009.03.007.

Hudak, A.T., Crookston, N.L., Evans, J.S., Hall, D.E., and Falkowski, M.J. 2008. "Nearest neighbor imputation of species-level, plot-scale forest structure attributes from LiDAR data." *Remote Sensing of Environment*, Vol. 112 (No. 5): pp. 2232–2245. doi:10.1016/j.rse.2007.10.009.

Hyyppä, E., Kukko, A., Kaijaluoto, R., White, J.C., Wulder, M.A., Pyörälä, J., Liang, X., *et al.* 2020. "Accurate derivation of stem curve and volume using backpack mobile laser scanning." *ISPRS Journal of Photogrammetry and Remote Sensing*, Vol. 161 pp. 246–262. doi:10.1016/j.isprsjprs.2020.01.018.

Jopia, A., Zambrano, F., Pérez-Martínez, W., Vidal-Páez, P., Molina, J., and De La Hoz Mardones, F. 2020. "Time-series of vegetation indices (VNIR/SWIR) derived from Sentinel-2 (A/B) to assess turgor pressure in Kiwifruit." *ISPRS International Journal of Geo-Information*, Vol. 9 (No. 11): pp. 641. doi:10.3390/ijgi9110641.

Kempeneers, P., and Soille, P. 2017. "Optimizing Sentinel-2 image selection in a Big Data context." *Big Earth Data*, Vol. 1 (No. 1-2): pp. 145–158. doi:10.1080/20964471.2017.1407489.

Kerr, J.T., and Deguise, I. 2004. "Habitat loss and the limits to endangered species recovery." *Ecology Letters*, Vol. 7 (No. 12): pp. 1163–1169. doi:10.1111/j.1461-0248.2004.00676.x.

LeDell, E., Petersen, M., and Van Der Laan, M. 2015. "Computationally efficient confidence intervals for cross-validated area under the ROC curve estimates." *Electronic Journal of Statistics*, Vol. 9 (No. 1): pp. 1583–1607. doi:10.1214/15-EJS1035.

Lefsky, M.A., Hudak, A.T., Cohen, W.B., and Acker, S.A. 2005. "Patterns of covariance between forest stand and canopy structure in the Pacific Northwest." *Remote Sensing of Environment*, Vol. 95 (No. 4): pp. 517–531. doi:10.1016/j.rse.2005.01.004.

Likens, G. E. (Ed.) 1989. *Long-Term Studies in Ecology*. Springer Science & Business Media. doi: 10.1007/978-1-4615-7358-6_5

Ma, Q., Su, Y., Niu, C., Ma, Q., Hu, T., Luo, X., Tai, X., *et al.* 2023. "Tree mortality during long-term droughts is lower in structurally complex forest stands." *Nature Communications*, Vol. 14 (No. 1): pp. 7467. doi:10.1038/s41467-023-43083-8.

MacKenzie, W.H., and Meidinger, D.V. 2018. "The Biogeoclimatic Ecosystem Classification Approach: An ecological framework for vegetation classification." *Phytocoenologia*, Vol. 48 (No. 2): pp. 203–213. doi:10.1127/phyto/2017/0160.

Maltman, J.C., Coops, N.C., Rickbeil, G.J.M., Hermosilla, T., and Burton, A.C. 2024. "Quantifying forest disturbance regimes within caribou (Rangifer tarandus) range in British Columbia." *Scientific Reports*, Vol. 14 (No. 1): pp. 6520. doi:10.1038/s41598-024-56943-0.

Maltman, J.C., Hermosilla, T., Wulder, M.A., Coops, N.C., and White, J.C. 2023. "Estimating and mapping forest age across Canada's forested ecosystems." *Remote Sensing of Environment*, Vol. 290 pp. 113529. doi:10.1016/j.rse.2023.113529.

Matasci, G., Hermosilla, T., Wulder, M.A., White, J.C., Coops, N.C., Hobart, G.W., Bolton, D.K., Tompalski, P., and Bater, C.W. 2018. "Three decades of forest structural dynamics over Canada's forested ecosystems using Landsat time-series and lidar plots." *Remote Sensing of Environment*, Vol. 216 pp. 697–714. doi:10.1016/j.rse.2018.07.024.

Maynard, D.G., Paré, D., Thiffault, E., Lafleur, B., Hogg, K.E., and Kishchuk, B. 2014. "How do natural disturbances and human activities affect soils and tree nutrition and growth in the Canadian boreal forest?" *Environmental Reviews*, Vol. 22 (No. 2): pp. 161–178. doi:10.1139/er-2013-0057.

Meddens, A.J.H., Hicke, J.A., Vierling, L.A., and Hudak, A.T. 2013. "Evaluating methods to detect bark beetle-caused tree mortality using single-date and multi-date Landsat imagery." *Remote Sensing of Environment*, Vol. 132 pp. 49–58. doi:10.1016/j.rse.2013.01.002.

Meidinger, D., & Pojar, J. (Eds.) 1991. Ecosystems of British Columbia (342 p). Special Report Series 6, Victoria, BC: B.C. Ministry of Forests and Range Research Branch.

Morin-Bernard, A., Achim, A., and Coops, N.C. 2023. "Attributing a causal agent and assessing the severity of non-stand replacing disturbances in a Northern Hardwood Forest using Landsat derived vegetation indices." *Canadian Journal of Remote Sensing*, Vol. 49 (No. 1): pp. 2196356. doi:10.1080/07038992.2023.2196356.

Mulverhill, C., Coops, N.C., and Achim, A. 2023. "Continuous monitoring and sub-annual change detection in high-latitude forests using Harmonized Landsat Sentinel-2 data." *ISPRS Journal of Photogrammetry and Remote Sensing*, Vol. 197 pp. 309–319. doi:10.1016/j.isprsjprs.2023.02.002.

Mulverhill, C., Coops, N.C., White, J.C., Tompalski, P., and Achim, A. 2025. "Evaluating the potential for continuous update of enhanced forest inventory attributes using optical satellite data." *Forestry: An International Journal of Forest Research*, Vol. 98 (No. 2): pp. 253–265. cpae029 doi:10.1093/forestry/cpae029.

Næsset, E. 2002. "Predicting forest stand characteristics with airborne scanning laser using a practical two-stage procedure and field data." *Remote Sensing of Environment*, Vol. 80 (No. 1): pp. 88–99. doi:10.1016/S0034-4257(01)00290-5.

NASA. 2024. "LP DAAC data resources." https://github.com/nasa/LPDAAC-Data-Resources

Nilsson, M. 1996. "Estimation of tree heights and stand volume using an airborne lidar system." *Remote Sensing of Environment*, Vol. 56 (No. 1): pp. 1–7. doi:10.1016/0034-4257(95)00224-3.

Nguyen, T., Jones, S., Soto-Berelov, M., Haywood, A., and Hislop, S. 2019. "Landsat time-series for estimating forest aboveground biomass and its dynamics across space and time: A review." *Remote Sensing*, Vol. 12 (No. 1): pp. 98. doi:10.3390/rs12010098.

Nlungu-Kweta, P., Leduc, A., and Bergeron, Y. 2017. "Climate and disturbance regime effects on aspen (*Populus tremuloides* Michx.) stand structure and composition along an east–west transect in Canada's boreal forest." *Forestry*, Vol. 90 (No. 1): pp. 70–81. doi:10.1093/forestry/cpw026.

Oliver, C. D., and Larson, B. A. 1996. *Forest Stand Dynamics* (Update ed.). Yale School of the Environment. https://elischolar.library.yale.edu/fes_pubs/1

Pasquarella, V., Bradley, B., and Woodcock, C. 2017. "Near-real-time monitoring of insect defoliation using Landsat time series." *Forests*, Vol. 8 (No. 8): pp. 275. doi:10.3390/f8080275.

Payette, S., Filion, L., and Delwaide, A. 1990. "Disturbance regime of a cold temperate forest as deduced from tree-ring patterns: the Tantaré Ecological Reserve, Quebec." *Canadian Journal of Forest Research*, Vol. 20 (No. 8): pp. 1228–1241. doi:10.1139/x90-162.

Pedregosa, F., Pedregosa, F., Varoquaux, G., Varoquaux, G., Org, N., Gramfort, A., Gramfort, A., *et al.* 2011. Scikit-learn: Machine Learning in Python. MACHINE LEARNING IN PYTHON.

Peng, C., Ma, Z., Lei, X., Zhu, Q., Chen, H., Wang, W., Liu, S., Li, W., Fang, X., and Zhou, X. 2011. "A drought-induced pervasive increase in tree mortality across Canada's boreal forests." *Nature Climate Change*, Vol. 1 (No. 9): pp. 467–471. doi:10.1038/nclimate1293.

Peters, M.I., and Despland, E. 2006. "Plasticity in forest tent caterpillar collective foraging schedules." *Ethology*, Vol. 112 (No. 6): pp. 521–528. doi:10.1111/j.1439-0310.2005.01197.x.

Pojar, J., Klinka, K., and Meidinger, D.V. 1987. "Biogeoclimatic ecosystem classification in British Columbia." *Forest Ecology and Management*, Vol. 22 (No. 1-2): pp. 119–154. doi:10.1016/0378-1127(87)90100-9.

R Core Team 2024. *R: A language and environment for statistical computing*. Vienna, Austria: R Foundation for Statistical Computing, https://www.R-project.org/.

Raab, C., Tonn, B., Meißner, M., Balkenhol, N., and Isselstein, J. 2019. "Multi-temporal rapideye tasselled cap data for land cover classification." *European Journal of Remote Sensing*, Vol. 52 (No. 1): pp. 653–666. doi:10.1080/22797254.2019.1701560.

RIEGL 2013. *RIEGL LMS-Q1560 datasheet* (LMS-Q1560). RIEGL. https://www.rieglusa.com/wp-content/uploads/lms-q1560-datasheet.pdf

Robin, X., Turck, N., Hainard, A., Tiberti, N., Lisacek, F., Sanchez, J.-C., and Müller, M. 2011. "pROC: An open-source package for R and S+to analyze and compare ROC curves." *BMC Bioinformatics*, Vol. 12 (No. 1): pp. 77. doi:10.1186/1471-2105-12-77.

Roberts, D.R., Bahn, V., Ciuti, S., Boyce, M.S., Elith, J., Guillera-Arroita, G., Hauenstein, S., *et al.* 2017. "Cross-validation strategies for data with temporal, spatial, hierarchical, or phylogenetic structure." *Ecography*, Vol. 40 (No. 8): pp. 913–929. doi:10.1111/ecog.02881.

Roussel, J.-R., and Auty, D. 2016. *lidR: Airborne LiDAR Data Manipulation and Visualization for Forestry Applications* (p. 4.1.2) [Dataset]. doi:10.32614/CRAN.package.lidR.

Roussel, J.-R., Auty, D., Coops, N.C., Tompalski, P., Goodbody, T.R.H., Meador, A.S., Bourdon, J.-F., de Boissieu, F., and Achim, A. 2020. "lidR: An R package for analysis of Airborne Laser Scanning (ALS) data." *Remote Sensing of Environment*, Vol. 251 pp. 112061. doi:10.1016/j.rse.2020.112061.

Senf, C., Seidl, R., and Hostert, P. 2017. "Remote sensing of forest insect disturbances: Current state and future directions." *International Journal of Applied Earth Observation and Geoinformation: ITC Journal*, Vol. 60: pp. 49–60. doi:10.1016/j.jag.2017.04.004.

Schroeder, T.A., Wulder, M.A., Healey, S.P., and Moisen, G.G. 2011. "Mapping wildfire and clearcut harvest disturbances in boreal forests with Landsat time series data." *Remote Sensing of Environment*, Vol. 115 (No. 6): pp. 1421–1433. doi:10.1016/j.rse.2011.01.022.

Smith-Tripp, S.M., Coops, N.C., Mulverhill, C., White, J.C., and Axelson, J. 2024. "Landsat assessment of variable spectral recovery linked to post-fire forest structure in dry sub-boreal forests." *ISPRS Journal of Photogrammetry and Remote Sensing*, Vol. 208: pp. 121–135. doi:10.1016/j.isprsjprs.2024.01.008.

Solberg, S., Næsset, E., Hanssen, K.H., and Christiansen, E. 2006. "Mapping defoliation during a severe insect attack on Scots pine using airborne laser scanning." *Remote Sensing of Environment*, Vol. 102 (No. 3-4): pp. 364–376. doi:10.1016/j.rse.2006.03.001.

Srivastava, V., and Carroll, A.L. 2023. "Dynamic distribution modelling using a native invasive species, the mountain pine beetle." *Ecological Modelling*, Vol. 482 pp. 110409. doi:10.1016/j.ecolmodel.2023.110409.

Swanson, M.E., Franklin, J.F., Beschta, R.L., Crisafulli, C.M., DellaSala, D.A., Hutto, R.L., Lindenmayer, D.B., and Swanson, F.J. 2011. "The forgotten stage of forest succession: Early-successional ecosystems on forest sites." *Frontiers in Ecology and the Environment*, Vol. 9 (No. 2): pp. 117–125. doi:10.1890/090157.

Thompson, I.D., Maher, S.C., Rouillard, D.P., Fryxell, J.M., and Baker, J.A. 2007. "Accuracy of forest inventory mapping: Some implications for boreal forest management." *Forest Ecology and Management*, Vol. 252 (No. 1-3): pp. 208–221. doi:10.1016/j.foreco.2007.06.033.

Tompalski, P., Coops, N.C., White, J.C., Goodbody, T.R.H., Hennigar, C.R., Wulder, M.A., Socha, J., and Woods, M.E. 2021. "Estimating changes in forest attributes and enhancing growth projections: A review of existing

approaches and future directions using airborne 3D point cloud data." *Current Forestry Reports*, Vol. 7 (No. 1): pp. 1–24. doi:10.1007/s40725-021-00135-w.

Trotto, T., Coops, N.C., Achim, A., Gergel, S.E., and Roeser, D. 2024. "Characterizing forest structural changes in response to non-stand replacing disturbances using bitemporal airborne laser scanning data." *Science of Remote Sensing*, Vol. 10 pp. 100160. doi:10.1016/j.srs.2024.100160.

Trumbore, S., Brando, P., and Hartmann, H. 2015. "Forest health and global change." *Science (New York, N.Y.)*, Vol. 349 (No. 6250): pp. 814–818. doi:10.1126/science.aac6759.

Vatandaslar, C., Lee, T., Bettinger, P., Ucar, Z., Stober, J., and Peduzzi, A. 2024. "Mapping percent canopy cover using individual tree- and area-based procedures that are based on airborne LiDAR data: Case study from an oak-hickory-pine forest in the USA." *Ecological Indicators*, Vol. 167: pp. 112710. doi:10.1016/j.ecolind.2024.112710.

Viana-Soto, A., García, M., Aguado, I., and Salas, J. 2022. "Assessing post-fire forest structure recovery by combining LiDAR data and Landsat time series in Mediterranean pine forests." *International Journal of Applied Earth Observation and Geoinformation*, Vol. 108: pp. 102754. doi:10.1016/j.jag.2022.102754.

Wagner, D., and Doak, P. 2013. "Long-term impact of a leaf miner outbreak on the performance of quaking aspen." *Canadian Journal of Forest Research*, Vol. 43 (No. 6): pp. 563–569. doi:10.1139/cjfr-2012-0486.

Wallace, B., Bulmer, C., Hope, G., Curran, M., Philpott, T., and Murray, M. 2021. "Soil compaction and organic matter removal effects on soil properties and tree growth in the Interior Douglas-fir zone of southern British Columbia." *Forest Ecology and Management*, Vol. 494: pp. 119268. doi:10.1016/j.foreco.2021.119268.

Wang, T., Hamann, A., Spittlehouse, D., and Carroll, C. 2016. "Locally Downscaled and Spatially Customizable Climate Data for Historical and Future Periods for North America." *PloS One*, Vol. 11 (No. 6): pp. e0156720. doi:10.1371/journal.pone.0156720.

Westfall, J., Ebata, T., and Hr GISolutions, I. 2019. Forest Health Aerial Overview Survey Standards for British Columbia.

White, J.C., Tompalski, P., Bater, C.W., Wulder, M.A., Fortin, M., Hennigar, C., Robere-McGugan, G., Sinclair, I., and White, R. 2025. "Enhanced forest inventories in Canada: Implementation, status, and research needs." *Canadian Journal of Forest Research*, Vol. 55: pp. 1–37. doi:10.1139/cjfr-2024-0255.

White, J.C., Wulder, M.A., Hobart, G.W., Luther, J.E., Hermosilla, T., Griffiths, P., Coops, N.C., *et al.* 2014. "Pixel-Based Image Compositing for Large-Area Dense Time Series Applications and Science." *Canadian Journal of Remote Sensing*, Vol. 40 (No. 3): pp. 192–212. doi:10.1080/07038992.2014.945827.

White, J.C., Wulder, M.A., Varhola, A., Vastaranta, M., Coops, N.C., Cook, B.D., Pitt, D., and Woods, M. 2013. "A best practices guide for generating forest inventory attributes from airborne laser scanning data using an area-based approach." *The Forestry Chronicle*, Vol. 89 (No. 06): pp. 722–723. doi:10.5558/tfc2013-132.

Woo, H., Eskelson, B.N.I., and Monleon, V.J. 2021. "Matching methods to quantify wildfire effects on forest carbon mass in the U.S. Pacific Northwest." *Ecological Applications: a Publication of the Ecological Society of America*, Vol. 31 (No. 3): pp. e02283. doi:10.1002/eap.2283.

Woods, K. D. 2000. Dynamics in Late-Successional Hemlock-Hardwood Forests over Three Decades.

Woods, K.D., and Kern, C.C. 2022. "Intermediate disturbances drive long-term fluctuation in old-growth forest biomass: An 84-yr temperate forest record." *Ecosphere*, Vol. 13 (No. 1): pp. e03871. doi:10.1002/ecs2.3871.

Wotherspoon, A.R., Achim, A., and Coops, N.C. 2024. "Assessing future climate trends and implications for managed forests across Canadian ecozones." *Canadian Journal of Forest Research*, Vol. 54 (No. 3): pp. 278–289. doi:10.1139/cjfr-2023-0058.

Ye, S., Rogan, J., Zhu, Z., and Eastman, J.R. 2021. "A near-real-time approach for monitoring forest disturbance using Landsat time series: stochastic continuous change detection." *Remote Sensing of Environment*, Vol. 252: pp. 112167. doi:10.1016/j.rse.2020.112167.

Yue, C., Kahle, H.-P., Klädtke, J., and Kohnle, U. 2023. "Forest stand-by-environment interaction invalidates the use of space-for-time substitution for site index modeling under climate change." *Forest Ecology and Management*, Vol. 527: pp. 120621. doi:10.1016/j.foreco.2022.120621.

Zald, H.S.J., Wulder, M.A., White, J.C., Hilker, T., Hermosilla, T., Hobart, G.W., and Coops, N.C. 2016. "Integrating Landsat pixel composites and change metrics with lidar plots to predictively map forest structure and aboveground biomass in Saskatchewan, Canada." *Remote Sensing of Environment*, Vol. 176: pp. 188–201. doi:10.1016/j.rse.2016.01.015.

Zhao, K., Wulder, M.A., Hu, T., Bright, R., Wu, Q., Qin, H., Li, Y., *et al.* 2019. "Detecting change-point, trend, and seasonality in satellite time series data to track abrupt changes and nonlinear dynamics: A Bayesian ensemble algorithm." *Remote Sensing of Environment*, Vol. 232: pp. 111181. doi:10.1016/j.rse.2019.04.034.